Search for a light muon-philic Z' with the NA64-e experiment at CERN

Yu. M. Andreev,[1] A. Antonov,[2] D. Banerjee,[3] B. Banto Oberha
M. Bondí,[6] A. Celentano,[2] N. Charitonidis,[3] D. Cooke,[7] P. Crivel
S. V. Donskov,[1] R. R. Dusaev,[1] T. Enik,[8] V. N. Frolov,[8] A. Gardik ,[10]
V. A. Kachanov,[1] Y. Kambar,[8] A. E. Karneyeu,[1] G. Kekelidze,
M. M. Kirsanov,[1] V. N. Kolosov,[1] S. V. Gertsenberger,[8] S. Girod,[3] E [1,8]
L. V. Kravchuk,[1] N. V. Krasnikov,[1,8] S. V. Kuleshov,[11,12] V. E. Lyub ,[2]
L. Marsicano,[2,*] V. A. Matveev,[8] R. Mena Fredes,[12] R. Mena Yanssen ,[4]
D. V. Peshekhonov,[8] V. A. Polyakov,[1] B. Radics,[15] K. Salamatin, V. D. Samoylenko, H. Sieber,
D. Shchukin,[1] O. Soto,[12,16] V. O. Tikhomirov,[1] I. Tlisova,[1] A. N. Toropin,[1] M. Tuzi,[14] P. Ulloa,[11]
P. V. Volkov,[1,8] V. Yu. Volkov,[1,†] I. V. Voronchikhin,[1] J. Zamora-Saá,[11,12] and A. S. Zhevlakov[8]

[1] *Authors affiliated with an institute covered by a cooperation agreement with CERN*
[2] *INFN, Sezione di Genova, 16147 Genova, Italia*
[3] *CERN, European Organization for Nuclear Research, CH-1211 Geneva, Switzerland*
[4] *ETH Zürich, Institute for Particle Physics and Astrophysics, CH-8093 Zürich, Switzerland*
[5] *Università degli Studi di Genova, 16126 Genova, Italia*
[6] *INFN, Sezione di Catania, 95125 Catania, Italia*
[7] *UCL Departement of Physics and Astronomy, University College London,*
Gower St. London WC1E 6BT, United Kingdom
[8] *Authors affiliated with an international laboratory covered by a cooperation agreement with CERN*
[9] *Physics Department, University of Patras, 265 04 Patras, Greece*
[10] *Universität Bonn, Helmholtz-Institut für Strahlen-und Kernphysik, 53115 Bonn, Germany*
[11] *Center for Theoretical and Experimental Particle Physics, Facultad de Ciencias Exactas,*
Universidad Andres Bello, Fernandez Concha 700, Santiago, Chile
[12] *Millennium Institute for Subatomic Physics at High-Energy Frontier (SAPHIR), Fernandez Concha 700, Santiago, Chile*
[13] *Universidad Técnica Federico Santa María and CCTVal, 2390123 Valparaíso, Chile*
[14] *Instituto de Fisica Corpuscular (CSIC/UV), Carrer del Catedratic Jose Beltran Martinez, 2, 46980 Paterna, Valencia, Spain*
[15] *Department of Physics and Astronomy, York University, Toronto, ON, Canada*
[16] *Departamento de Fisica, Facultad de Ciencias,*
Universidad de La Serena, Avenida Cisternas 1200, La Serena, Chile

CERN-EP-2024-103
09 April 2024

(Dated: April 8, 2024)

The inclusion of an additional $U(1)$ gauge $L_\mu - L_\tau$ symmetry would release the tension between the measured and the predicted value of the anomalous muon magnetic moment: this paradigm assumes the existence of a new, light Z' vector boson, with dominant coupling to μ and τ leptons and interacting with electrons via a loop mechanism. The $L_\mu - L_\tau$ model can also explain the Dark Matter relic abundance, by assuming that the Z' boson acts as a "portal" to a new Dark Sector of particles in Nature, not charged under known interactions. In this work we present the results of the Z' search performed by the NA64-e experiment at CERN SPS, that collected $\sim 9 \times 10^{11}$ 100 GeV electrons impinging on an active thick target. Despite the suppressed Z' production yield with an electron beam, the limits sets by NA64-e are competitive with other experimental searches, and partially exclude the g-2 preferred model parameter values for Z' masses lighter than 2 MeV. This result proves the complementarity of this search with NA64-μ, the parallel effort of the NA64 collaboration with a muon beam.

Introduction The Standard Model (SM) of fundamental interactions is one the greatest successes of particle physics, explaining many phenomena at different energy scales. Despite these results, the SM needs to be extended to account for several experimentally observed anomalies or effects, currently not described by the model. A remarkable example is provided by the Dark Matter (DM) particle content puzzle. Nowadays, the existence of DM is confirmed by multiple astrophysical and cosmological observations, but the SM does not include any viable DM particle candidate [? ? ?]. This calls for an extension of the SM, with new fields and forces not yet experimentally observed [?]. Another significant example is provided by the measurement of the anomalous muon magnetic moment $a_\mu \equiv (g_\mu - 2)/2$. For this observable, the most updated experimental average, mostly constrained by the latest Fermilab Muon $g-2$ experiment, reads $a_\mu(\mathrm{Exp}) = 116\,592\,059(22) \times 10^{-11}$ [1], to be compared with the latest theoretical prediction from the Muon $g-2$ Theory Initiative, $a_\mu(\mathrm{Teo}) = 116\,591\,810(43) \times 10^{-11}$ [2]. The leading order hadronic contribution for a_μ comes from the cross section for the $e^+e^- \to$ hadrons process, measured by many experiments. While new results from both the experimental side (e.g., the latest CMD-3 result [3], still unpublished) and the phenomenological one (e.g., a recent lattice calculation by the BMW collaboration [4]) tend to reduce the experiment-to-theory discrepancy, still this difference motivates the investigation of new physics scenarios with a preferred connection to SM second generation leptons.

The $L_\mu - L_\tau$ model. A possible model releasing this tension can be constructed by gauging the $L_\mu - L_\tau$ combination; this naturally predicts the existence of a new $U(1)$ gauge boson, Z', that couples to second and third generation leptons via a coupling $g_{Z'}$ [5, 6]. The corresponding new Lagrangian terms read [7]:

$$\begin{aligned}\mathcal{L} \subset & -\frac{1}{4}{Z'}_{\mu\nu}{Z'}^{\mu\nu} + \frac{1}{2}m_{Z'}^2 {Z'}_\mu {Z'}^\mu \\ & - g_{Z'}{Z'}_\mu \left(\bar{\mu}\gamma^\mu\mu + \bar{\nu}_\mu\gamma^\mu P_L\nu_\mu - \bar{\tau}\gamma^\mu\tau - \bar{\nu}_\tau\gamma^\mu P_L\nu_\tau\right) \quad ,\end{aligned} \tag{1}$$

where $Z'_{\mu\nu} \equiv \partial_\mu {Z'}_\nu - \partial_\nu {Z'}_\mu$ is the Z' field strength, $m_{Z'}$ is the Z' mass, and $P_L = (1-\gamma_5)/2$. In this model, loop-order effects generate an additional positive contribution to a_μ(Theo), bringing it closer to a_μ(Exp). In particular, for values $g_{Z'} \simeq 4.5 \times 10^{-4}$ and $m_{Z'} \ll m_\mu$, the Z' contribution would actually solve the muon $g-2$ discrepancy. Recently, results from the search of a Z' boson decaying to muons have been reported by the BaBar [26], Belle [**?**], Belle-II [**?**], and CMS [**?**] experiments, with null observations so far. The same result was reported by Belle-II from the search of an invisibly-decaying Z' [27].

The model can also be connected to the DM phenomenology in the context of Dark Sector (DS) scenarios, by postulating the existence of a new ensemble of particles in Nature, not charged under SM interactions. The lightest particle of the DS (here denoted as χ), if stable, can be the DM candidate. Assuming, for illustration, a complex scalar nature for the χ, the Lagrangian is extended by the $Z' - \chi$ interaction term $\mathcal{L}_D = g_D {Z'}_\mu J^\mu_D$, where $J^\mu_D = (\chi^* i\partial^\mu\chi - \chi i\partial^\mu\chi^*)$ is the DS current and $g_D \equiv \sqrt{4\pi\alpha_D}$ is the coupling constant. In this picture, considering the mass hierarchy $m_{Z'} > m_\chi$, and far from the resonance condition $m_{Z'} = 2m_\chi$, the presently observed DM relic abundance is set by the velocity-averaged cross section for the process $l\bar{l} \to Z' \to \chi\chi$, where l is a SM lepton, if DM had a thermal origin in the early Universe. This results to a preferred combination of the model parameters related as [8]:

$$g_D^2 g_{Z'}^2 \left(\frac{m_\chi}{m_{Z'}}\right)^4 \simeq 3 \cdot 10^{-15} \left(\frac{m_\chi}{1\,\mathrm{MeV}}\right)^2 \quad . \tag{2}$$

As discussed in Ref. [9], even if the $L_\mu - L_\tau$ model does not explicitly include a tree-level coupling between electrons and the Z', this is straightforwardly introduced via the one-loop level kinetic mixing between the Z' and the photon, resulting to the effective coupling $e\Pi(q^2)$ dependent on the momentum squared q^2 carried by the Z' [10–12][1]:

$$\Pi(q^2) = \frac{e\,g_{Z'}}{2\pi^2}\int_0^1 dx\, x(1-x)\ln\frac{m_\tau^2 - x(1-x)q^2}{m_\mu^2 - x(1-x)q^2} \quad . \tag{3}$$

In particular, for $q^2 \ll m_\mu^2$, the loop function $\Pi(q^2)$ approaches to $\Pi(q^2) \simeq \Pi(0) = \frac{e\,g_{Z'}}{6\pi^2}\ln\frac{m_\tau}{m_\mu} \simeq 0.014 \cdot g_{Z'}$, and the phenomenology of the $L_\mu - L_\tau$ model is similar to that of a dark photon model [13], with the substitution $\varepsilon = 0.0144 \cdot g_{Z'}$, with ε being the kinetic mixing parameter. At large q^2, $|\Pi(q^2)|$ grows, reaching a maximum value $\simeq 0.021 g_{Z'}$ at $q^2 = m_\mu^2$, and then smoothly goes to zero for $q^2 \gg 0$.

The Z' search at NA64$-e$. Due to the loop-induced effective coupling, the Z' paradigm can be explored at electron-beam experiments. In this work, we present the latest results of the search for the Z' particle at the NA64$-e$ experiment at CERN SPS. In a collision of a high-energy electron beam with a thick target, Z' particles can be produced by two main processes involving the primary electron and the secondaries produced in the electromagnetic cascade, namely the radiative emission (Z'-strahlung) in the electromagnetic field of an atom by an electron/positron, $e^\pm N \to e^\pm N Z'$, and the resonant annihilation of a secondary positron with an atomic electron, $e^+e^- \to Z'$. Depending on the mass and on the couplings, the produced Z' will then decay to one of the allowed dominant channels, i.e. $\mu^+\mu^-$, $\tau^+\tau^-$, $\nu\bar{\nu}$, or $\chi\chi$, where the neutrino channel refers both to ν_μ and ν_τ. NA64$-e$ exploits the *invisible* decay channel ($\nu\bar{\nu}$ or $\chi\chi$) to investigate the Z' existence by relying on the missing-energy technique with a E_0 =100 GeV electron beam impinging on an active thick target. The signature for the Z' production, followed by its invisible decay, is the observation of events with a well identified impinging e^- track, in coincidence with a large missing energy E_{miss}, measured as the difference between the nominal beam energy E_0 and the one deposited in the active target E_{ECAL}, and no activity in the other downstream apparatus [14]. A schematic representation of the NA64$-e$ detector assembly is shown in Fig. 1. Incoming particles are detected by a set of three plastic scintillator counters (S1, S2, S3) and two veto counters (V1, V2). A magnetic spectrometer, consisting of tracking detectors (GEMs, MicroMegas, and Straw Tubes) placed upstream and downstream two dipole magnets (MBPL 1, MBPL 2) with a combined magnetic strength of approximately 7 T·m, is utilized for measuring particle momentum, with a resolution $\delta p/p$ of about 1% [15]. Particle identification is achieved by detecting synchrotron radiation (SR) photons emitted by the electrons deflected by the magnetic field through a compact Pb/Sc calorimeter

---

[1] The full analytic expression for $\Pi(q^2)$ can be found in the Appendix of Ref. [9] Appendix.

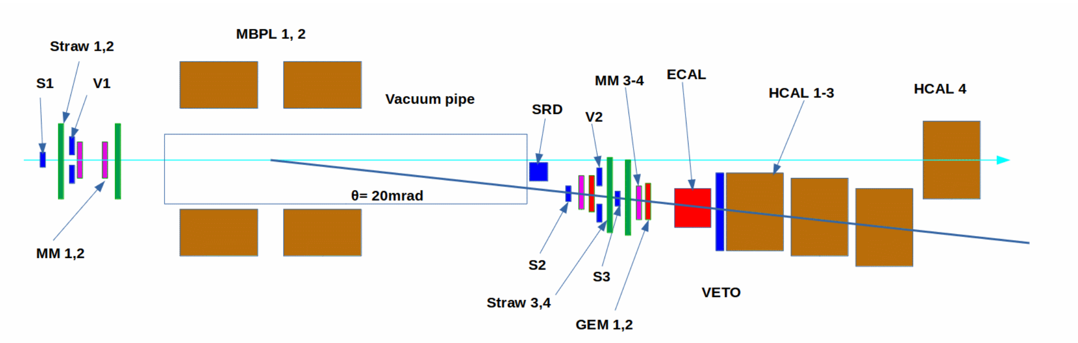

FIG. 1. Schematic representation of the NA64$-e$ detector, searching for an invisibly decaying Z' produced by the interaction of 100 GeV electrons with the material of the active ECAL target. See text for further details.

(SRD) [16]. The NA64 active target is a Pb/Sc calorimeter (ECAL) with a thickness of 40 X_0, organized in a 5×6 matrix of 3.82×3.82 cm^2 cells. Each cell has independent PMT readout and is longitudinally segmented into a 4 X_0 pre-shower section and a main section. Following the ECAL, a hermetic Fe/Sc hadron calorimeter (HCAL) with three modules, totaling approximately 21 λ_I in length, is installed to detect secondary hadrons and muons produced in the ECAL and upstream beamline elements. A fourth module is installed at zero degrees, to capture neutral particles produced by the beam interacting with upstream materials. A high-efficiency plastic scintillator counter (VETO) is placed between the ECAL and HCAL to further reduce background signals. The trigger for the experiment required the coincidence between signals from the scintillator counters, in anti-coincidence with the veto detectors, paired with an in-time energy deposition in the calorimeter satisfying the constraints $E_{ECAL} \lesssim 90$ GeV, $E_{PRS} \gtrsim 300$ MeV [18].

Data analysis. The results here presented are based on a total statistics of $(9.1 \pm 0.5) \times 10^{11}$ electrons on target (EOT) accumulated in different runs by NA64$-e$ during the 2016-2022 period, with beam intensity up to $\simeq 6 \times 10^6$ electrons per SPS spill of 4.8 s. The data analysis was based on the same dataset already scrutinized and unblinded for the recently published invisibly-decaying dark photon search [17]. Therefore, supported by the fact that the phenomenology of an invisible-decaying Z' is very similar to that of the A' search, we decided to adopt the same reconstruction algorithms and event selection criteria, resulting in zero observed events in the signal window. The analysis required the presence of a well identified impinging electron with momentum 100 ± 10 GeV, paired with an in-time energy deposition in the SRD detector in the range $\simeq 1 - 100$ MeV. Events with electro- and photo-nuclear interactions in the ECAL were suppressed by requiring the compatibility of the measured energy deposition in the different cells, in terms of longitudinal and transverse shape, with that expected from an electron-induced electromagnetic shower [18]. No activity should be observed in the VETO and in the HCAL detector; for the latter, a 1 GeV energy threshold was set, just above the noise level. Finally, we adopted the same value of the ECAL missing energy threshold defining the signal box ($E_{ECAL} < E^{thr}_{ECAL}$) that was optimized independently for each particular run period, accounting for small differences in the detector response and in the observed background levels. Obtained values were in the range $E^{thr}_{ECAL} \sim 47 - 50$ GeV. The most critical background source was due to upstream interactions of the impinging particle with beamline materials, with the low-energy scattered electron hitting the ECAL and the secondary hadrons produced at large angle, outside the HCAL acceptance. To suppress it, a multiplicity cut on the measured number of hits in the STRAW detectors was used. The residual yield was evaluated directly from the data, considering events lying in the sideband region $E_{HCAL} \simeq 0$, $E_{ECAL} < E_0$, and extrapolating the corresponding ECAL energy distribution in the signal region through an exponential model. For the 2021-2022 runs, the expected background is (0.3 ± 0.2) events, where the error has been evaluated by varying the parameters of the model within their fit uncertainty and repeating the procedure. Secondary contributions arose from the in-flight decay of π^- and μ^- beam contaminants [19], estimated with Monte Carlo, as well as from the punch-through of leading neutral hadrons (n, K) produced in the ECAL, valuated from a dedicated measurement [20].

Signal simulation. The expected yield S of Z' events within the signal window for given values of the model parameters was computed using the DMG4 software [21, 24], integrated within the full Geant4-based simulation of the NA64$-e$ detector [**?** **?**]. We considered two model variations: a "vanilla" case in which $g_D = 0$ and a "dark sector" one featuring non-zero $Z' - \chi$ DS coupling, focusing on the $1\,\text{MeV} \lesssim m_{Z'} \lesssim 500\,\text{MeV}$ mass range for $g_{Z'} < 0.1$. For these parameters values, and in particular in the first scenario, the Z' width is very narrow [9]; this was appropriately treated in the simulation, as discussed in the following. Both the Z'-strahlung and

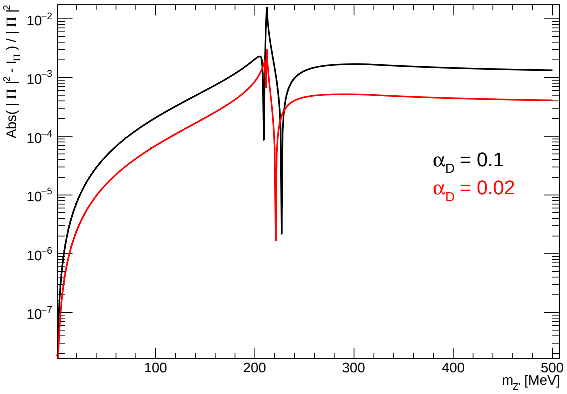

FIG. 2. The relative difference between the Π function on-shell value $|\Pi|^2$ and the q^2-averaged one $I_{|\Pi|^2}$ as a function of the Z' mass, for different α_D values.

the resonant annihilation production processes were implemented in DMG4, addressing the model peculiarities arising from the loop-induced $e^- - Z'$ coupling, as well the Z' width. We first considered the effects associated with the q^2 dependency of the Π function, starting from the Z'-strahlung process. In the "dark sector" case and for the $Z' \to \chi\chi$ decay channel, the cross-section expression contains an average $Z' - e^-$ kinetic mixing value $I_{|\Pi|^2}$ (see also Ref. [9], Eq. A.5):

$$I_{|\Pi|^2} = \int_{q^2_{min}}^{q^2_{max}} dq^2 \frac{\left|\Pi(q^2)\right|^2}{\pi} \frac{\sqrt{q^2}\,\Gamma_{Z'}}{(q^2 - m^2_{Z'})^2 + m^2_{Z'}\Gamma^2_{Z'}} , \quad (4)$$

where $q^2_{min} = 4m^2_\chi$ and $q^2_{max} \gg m^2_{Z'}$ in the NA64$-e$ kinematic regime. In Fig. 2, we compare $I_{|\Pi|^2}$ with the on-shell value $|\Pi(m^2_{Z'})|^2$, for $\alpha_D = 0.1$ (black curve) and $\alpha_D = 0.02$ (red curve), by showing the relative difference among the two as a function of the Z' mass[2]. As expected, the largest variation is seen for $m_{Z'} \simeq 2m_\mu$, since here the variation of the Π function with respect to q^2 is larger. We observe that, as a consequence of the narrow Z' width, the relative difference is always smaller than $\simeq$ 1%. This justifies the use of an on-shell approximation for the $Z'-$strahlung cross section, i.e. $I_{|\Pi|^2} \simeq |\Pi(m^2_{Z'})|^2$. The same conclusion holds for the "vanilla" scenario, given the even narrower Z' width. Finally, for the e^+e^- resonant production the full q^2 dependency of the Π function is naturally accounted for in the tree-level expression for $\sigma(s)$, where s is the e^+e^- invariant mass squared, given the identity $q^2 = s$ – see also Ref. [9], Eqs. (A.3) and (A.4).

A second critical effect considered in the simulation is the modification of the effective line shape for the e^+e^- annihilation channel due to the atomic electrons motion. This effect is well known in atomic physics, where it induces, for example, a broadening of the photon energy spectrum in the $e^+e^- \to \gamma\gamma$ reaction [22]. In particular, for in-flight annihilation atomic motions manifest as the appearance of events with $E_\gamma > E_{max}$, where E_{max} was the maximum allowed photon energy if the atomic electron was at rest [23]. To our knowledge, this effect has never been implemented in a full Monte Carlo simulation of the resonant production of DS states, although recently an analytical calculation was performed in Ref. [?] for the case of a $\simeq$ 280 MeV positron beam impinging on a thin target. Indeed, for a given positron energy E_+ in the reference frame of the target atom, the e^+e^- invariant mass is given by the expression $s = 2m^2_e + 2E_+(E_- - zP_-)$, being E_- (P_-) the electron energy (momentum), and z the cosine of the angle between the two leptons. This implies that if the energy of a positron does not align with the resonance mass when interacting with a stationary electron, it can still do so when annihilating with an orbiting electron, and vice versa. To account for this, we computed an average cross section per atom, starting from the tree-level expression for the annihilation cross section, given by the formula

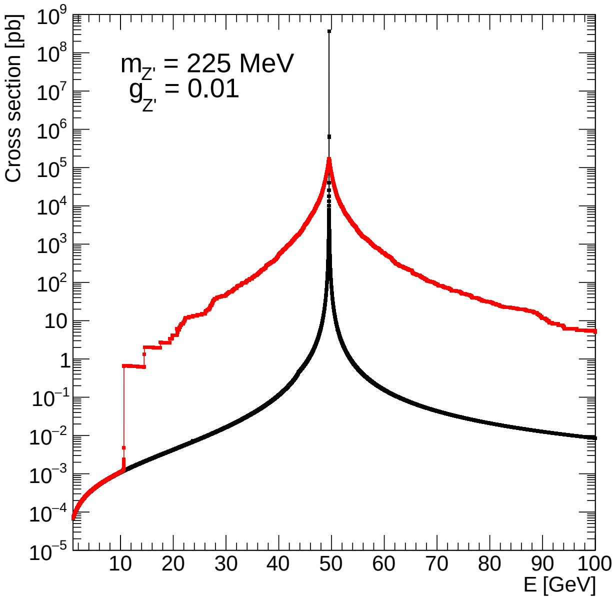

FIG. 3. Total atomic cross section for the process $e^+e^- \to Z' \to \nu\bar{\nu}$ on lead as a function of the impinging positron energy, considering (red) or not (black) the motion of atomic electrons.

$$\sigma = \frac{A(E_+)}{(2m^2_e + 2E_+(E_- - zP_-) - m^2_{Z'})^2 + m^2_{Z'}\Gamma^2_{Z'}} , \quad (5)$$

where $A(E_+)$ is a smooth-varying function of the impinging positron energy. We assumed a flat distribution

---

[2] In the DS case, the width $\Gamma_{Z'}$ is dominated by the α_D contribution; we therefore neglected its dependency on $g_{Z'}$.

for z and integrated over it to obtain an average value $\overline{\sigma}(E_+, E_-)$, depending solely on the positron and electron energy. Then, to integrate over E_-, we parameterized the kinetic energy distribution through a model inspired by the virial theorem, $\overline{T} = E_B$, where $-E_B$ is the binding energy, adopting an exponential ansatz $p(T_-) = \frac{1}{E_B}\exp(-T_-/E_B)$ [23], and then we summed over the contributions from each atomic shell [24]. For illustration, Fig. 3 shows the cross section per atom as a function of the positron energy for the reaction $e^+e^- \to Z' \to \nu\bar{\nu}$ on lead ("vanilla" case) when $m_{Z'} = 225$ MeV and $g_{A'} = 0.03$, comparing the result obtained with (red) and without (black) the atomic effects. We observe that, due to atomic effects, the cross section value at the peak is reduced by many orders of magnitude, and simultaneously the shape is significantly enlarged, keeping a constant value for the integral with respect to the positron energy across the allowed kinematic range.

After the Z' yield evaluation via simulation, we estimated the signal efficiency κ directly from the experimental data, applying the same selection cuts, except for the E^{thr}_{ECAL} threshold, to pure impinging electron events measured during calibration runs . The overall result reads $\kappa \simeq 50\%$, with a $\simeq 10\%$ variation between different runs mostly due to an increased beam intensity, and thus to a larger pile-up probability, for 2016 and 2022 periods. To account for the systematic uncertainty on the ECAL energy threshold, for each Z' mass value the procedure was repeated multiple times by sampling E^{thr}_{ECAL} from a Gaussian PDF, and then re-evaluating S. The RMS value of all results was taken as an estimate of ΔS. Finally, an additional 15% uncertainty on the absolute yield was also introduced to account for the observed difference on the number of "di-muon" events between data and Monte Carlo [17].

Results. Starting from the zero events measured in the signal window, the predicted background level B, and the simulated Z' yield, we computed an upper limit on the $g_{Z'}$ coupling as a function of $m_{Z'}$, for the cases $\alpha_D = 0$ ("vanilla") and $\alpha_D = 0.02$ / $\alpha_D = 0.1$ ("dark sector"). We used a frequentist method, considering the 90% Confidence Level (CL) of a one-sided profile-likelihood test statistics [25]. The likelihood model was built assuming a Poisson PDF for the number of events in the signal region, with mean value $\mu = S + B$. To handle the non-trivial dependency of S on $g_{Z'}$, entering both in the cross-section multiplicative pre-factor and in the Z' width [9], we proceeded by iteration, repeating at each time the computation of S via Monte Carlo and the extraction of the limit by adopting the $g_{Z'}$ value returned from the previous iteration. The first iteration was performed using the $g_{Z'}$ values reported in our previous work [9]. Convergence was observed already after three iterations.

The obtained results are shown in Fig. 4, reporting in red the 90% CL limit for the "vanilla" scenario (left plot) and for the "dark sector" one (right plot), with $\alpha_D = 0.1$ (continuous line) and $\alpha_D = 0.02$ (dashed line) and $m_{Z'}/m_\chi = 3$. In the same plots, we also show recent exclusion limits from BaBar [26] and Belle-II [27], as well as the latest result obtained by the NA64 collaboration through a dedicated missing-momentum experiment with a muon beam, NA64-μ [28]. Results from previous neutrinos experiments (CCFR [29] and Borexino [30]) are also reported – as already underlined in Ref. [31], these should be taken with care, being them a theoretical re-interpretation of the original experimental data. In both figures, the green band correspond to the preferred combination of the Z' parameters that would solve the muon $g-2$ tension. Finally, in the "dark sector" scenario, the black lines report the predicted value of $g_{Z'}$ as a function of the Z' mass from Eq. 2.

In conclusion, we performed the analysis of the data collected by NA64-e in the 2016-2022 period, searching for an invisibly decaying Z' boson. In the data analysis, we adopted the same selection criteria identified in the search for an invisibly decaying Dark Photon, resulting in zero observed events in the signal box. The signal yield was evaluated by means of MC simulation: the dominant Z' production mechanisms where implemented in the DMG4 software package, integrated in the Geant4-based MC framework of NA64-e, including the momentum-transfer dependency of the $Z' - e^-$ coupling and the effect of the motion of atomic electrons. Despite the disfavoured Z' production processes with an electron beam, the obtained limits prove to be complementary to the NA64-μ effort, touching the $g-2$ band in the low Z' mass. We underline that, apart from the re-analysis of data by Borexino, NA64-e sets the strongest limits for $m_{Z'} \lesssim 1.5$ MeV; the obtained limit for $m_{Z'} = 1$ MeV is $g_{Z' lim} = 3.8 \times 10^{-4}$, excluding almost all the $g-2$ band.

We gratefully acknowledge the support of the CERN management and staff, and the technical staffs of the participating institutions for their vital contributions. This result is part of a project that has received funding from the European Research Council (ERC) under the European Union's Horizon 2020 research and innovation programme, Grant agreement No. 947715 (POKER). This work was supported by the HISKP, University of Bonn (Germany), ETH Zurich and SNSF Grant No. 169133, 186181, 186158, 197346 (Switzerland), and FONDECYT (Chile) under Grant No. 1240066, and ANID - Millenium Science Initiative Program - ICN2019 044 (Chile), and RyC-030551-I and PID2021-123955NA-100 funded by MCIN/AEI/ 10.13039/501100011033/FEDER, UE (Spain).

---

[*] Corresponding author; luca.marsicano@ge.infn.it

[†] Deceased

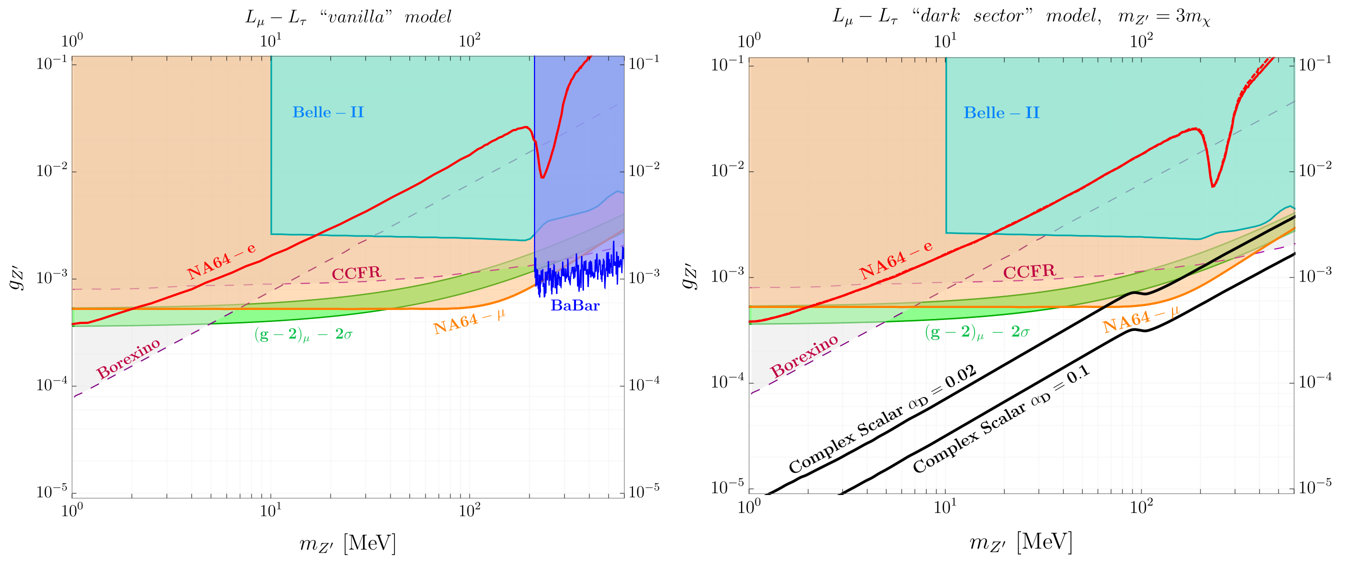

FIG. 4. The new exclusion limits from the NA64−e experiment in the $(g_{Z'}, m_{Z'})$ parameter space for the $L_\mu - L_\tau$ model, considering the "vanilla" scenario without any DS coupling (left) and the full "dark sector one" (right), for $\alpha_D = 0.1$ (continuous curve) and $\alpha_D = 0.02$ (dashed curve). The most competitive bounds reported by other experiments are also reported (see text for further details). The green band correspond to preferred combination of the model parameters that would solve the muon $g-2$ tension. Finally, the black curves in the right plot the preferred combination of the parameters to explain the observed dark matter relic density (so-called "thermal target").

[1] D. P. Aguillard *et al.* (Muon g-2), Phys. Rev. Lett. **131**, 161802 (2023), arXiv:2308.06230 [hep-ex].
[2] T. Aoyama *et al.*, Phys. Rept. **887**, 1 (2020), arXiv:2006.04822 [hep-ph].
[3] F. V. Ignatov *et al.* (CMD-3), (2023), arXiv:2302.08834 [hep-ex].
[4] S. Borsanyi *et al.*, Nature **593**, 51 (2021), arXiv:2002.12347 [hep-lat].
[5] X. G. He, G. C. Joshi, H. Lew, and R. R. Volkas, Phys. Rev. D **43**, 22 (1991).
[6] X.-G. He, G. C. Joshi, H. Lew, and R. R. Volkas, Phys. Rev. D **44**, 2118 (1991).
[7] M. Bauer, P. Foldenauer, and J. Jaeckel, JHEP **07**, 094, arXiv:1803.05466 [hep-ph].
[8] Y. Kahn, G. Krnjaic, N. Tran, and A. Whitbeck, JHEP **09**, 153, arXiv:1804.03144 [hep-ph].
[9] Y. M. Andreev *et al.* (NA64), Phys. Rev. D **106**, 032015 (2022), arXiv:2206.03101 [hep-ex].
[10] T. Araki, S. Hoshino, T. Ota, J. Sato, and T. Shimomura, Phys. Rev. D **95**, 055006 (2017), arXiv:1702.01497 [hep-ph].
[11] S. N. Gninenko and N. V. Krasnikov, Phys. Lett. B **783**, 24 (2018), arXiv:1801.10448 [hep-ph].
[12] Y. Zhang, Z. Yu, Q. Yang, M. Song, G. Li, and R. Ding, Phys. Rev. D **103**, 015008 (2021), arXiv:2012.10893 [hep-ph].
[13] M. Fabbrichesi, E. Gabrielli, and G. Lanfranchi (2020) SpringerBrief in Physics, arXiv:2005.01515 [hep-ph].
[14] S. N. Gninenko, N. V. Krasnikov, M. M. Kirsanov, and D. V. Kirpichnikov, Phys. Rev. D **94**, 095025 (2016), arXiv:1604.08432 [hep-ph].
[15] D. Banerjee *et al.*, Nucl. Instrum. Meth. A **881**, 72 (2018), arXiv:1708.04087 [physics.ins-det].
[16] E. Depero *et al.*, Nucl. Instrum. Meth. A **866**, 196 (2017), arXiv:1703.05993 [physics.ins-det].
[17] Y. M. Andreev *et al.* (NA64), Phys. Rev. Lett. **131**, 161801 (2023), arXiv:2307.02404 [hep-ex].
[18] D. Banerjee *et al.* (NA64), Phys. Rev. D **97**, 072002 (2018), arXiv:1710.00971 [hep-ex].
[19] Y. M. Andreev *et al.*, (2023), arXiv:2305.19411 [hep-ex].
[20] D. Banerjee *et al.* (NA64), Phys. Rev. Lett. **125**, 081801 (2020), arXiv:2005.02710 [hep-ex].
[21] M. Bondi, A. Celentano, R. R. Dusaev, D. V. Kirpichnikov, M. M. Kirsanov, N. V. Krasnikov, L. Marsicano, and D. Shchukin, Comput. Phys. Commun. **269**, 108129 (2021), arXiv:2101.12192 [hep-ph].
[22] V. J. Ghosh, M. Alatalo, P. Asoka-Kumar, B. Nielsen, K. G. Lynn, A. C. Kruseman, and P. E. Mijnarends, Phys. Rev. B **61**, 10092 (2000).
[23] A. W. Hunt, D. B. Cassidy, P. A. Sterne, T. E. Cowan, R. H. Howell, K. G. Lynn, and J. A. Golovchenko, Phys. Rev. Lett. **86**, 5612 (2001).
[24] B. B. Oberhauser *et al.*, (2024), arXiv:2401.12573 [hep-ph].
[25] E. Gross, in *PHYSTAT-LHC Workshop on Statistical Issues for LHC Physics* (2007).
[26] J. P. Lees *et al.* (BaBar), Phys. Rev. D **94**, 011102 (2016), arXiv:1606.03501 [hep-ex].
[27] I. Adachi *et al.* (Belle-II), Phys. Rev. Lett. **130**, 231801 (2023), arXiv:2212.03066 [hep-ex].
[28] H. Sieber, D. Banerjee, P. Crivelli, E. Depero, S. N. Gninenko, D. V. Kirpichnikov, M. M. Kirsanov, V. Poliakov, and L. Molina Bueno, Phys. Rev. D **105**, 052006 (2022), arXiv:2110.15111 [hep-ex].
[29] W. Altmannshofer, S. Gori, M. Pospelov, and I. Yavin, Phys. Rev. Lett. **113**, 091801 (2014), arXiv:1406.2332 [hep-ph].
[30] A. Kamada and H.-B. Yu, Phys. Rev. D **92**, 113004

(2015), arXiv:1504.00711 [hep-ph].

[31] S. Gninenko and D. Gorbunov, Phys. Lett. B **823**, 136739 (2021), arXiv:2007.16098 [hep-ph].